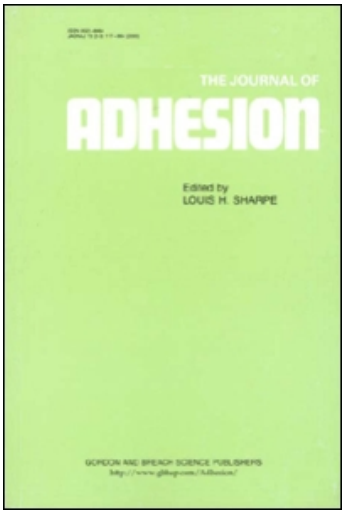

The Journal of Adhesion
Publication details, including instructions for authors and subscription information:
http://www.informaworld.com/smpp/title~content=t713453635

Effect of Deposition Conditions on Structure and Properties of Plasma-Polymerized Silica Primers

R. G. Dillingham[a]
[a] Brighton Technologies Group, Inc., Cincinnati, Ohio, USA

To cite this Article Dillingham, R. G.(2008) 'Effect of Deposition Conditions on Structure and Properties of Plasma-Polymerized Silica Primers', The Journal of Adhesion, 84: 8, 702 — 724
To link to this Article: DOI: 10.1080/00218460802352868
URL: http://dx.doi.org/10.1080/00218460802352868

The Journal of Adhesion, 84:702–724, 2008

ISSN: 0021-8464 print/1545-5823 online
DOI: 10.1080/00218460802352868

Taylor & Francis
Taylor & Francis Group

Effect of Deposition Conditions on Structure and Properties of Plasma-Polymerized Silica Primers

R. G. Dillingham
Brighton Technologies Group, Inc., Cincinnati, Ohio, USA

Plasma polymerized silica (PP-SiO_2) has been investigated as a surface pretreatment for adhesive bonding of metals. Strength and durability of adhesive joints prepared from PP-SiO_2 coated substrates using aerospace and automotive adhesives is excellent. However, epoxy adhesive systems based on primary amine curing agents do not perform well without further chemical derivatization of the PP-SiO_2. This work discusses the relationship between deposition conditions and primer structure as determined by FTIR and XPS and shows that curing agents containing primary amines are capable of catalyzing hydrolysis of silica in the near-interface regions in the presence of water. This hydrolysis does not occur with dicyandiamide-cured adhesives.

Keywords: Adhesive bonding; Durability; Interface; Plasma; Pretreatment

INTRODUCTION

Treatment of metal surfaces prior to adhesive bonding or painting is critical to the strength and durability of adhesively bonded structures such as found in automobiles and aircraft. Current metal pretreatment processes perform well, but generate tremendous volumes of environmentally damaging wastes such as hexavalent chromium, lead, and various inorganic acids. It may be possible to replace these environmentally damaging pretreatment processes in certain applications by engineering the metal surface with a vapor phase process, whereby the metal surface is first etched in a low temperature plasma, then coated with a thin film of plasma polymerized (PP)-SiO_2 [1–3].

Received 26 October 2007; in final form 16 May 2008.
One of a Collection of papers honoring John F. Watts, the recipient in February 2008 of *The Adhesion Society Award for Excellence in Adhesion Science, Sponsored by 3M*.
Address correspondence to R. G. Dillingham, Brighton Technologies Group, Inc., 1006 Kiely Place, Cincinnati, Ohio 45217. E-mail: gdillingham@btgnow.com

However, depending upon adhesive chemistry, the surface chemistry and morphology of the plasma polymerized films may need to be tailored to obtain strong and durable bonds with the desired adhesives.

In plasma processing, the surface of a solid is exposed to a low pressure gas under an applied electric field. A *plasma* results from collisions between free electrons and gas-phase molecules that form active species such as ions, free electrons, and radicals. If the gas is nonpolymerizing, the surface will be etched to remove low molecular weight organic contaminants. In the case of an organic polymer, the surface can be modified by addition of functional groups that increase the surface energy and improve wetting. In the case of a metal substrate, the surface oxide can be reduced or dehydrated. If the gas is capable of polymerizing, gas-phase species react with themselves and/or with the activated surface to form polymer films. The properties of plasma-polymerized films, including high crosslink density, high thermal stability, low gas/water vapor permeability, low conductivity, high abrasion and wear resistance, and excellent adhesion [4–10], are attractive as primers that can replace conventional metal pretreatments, such as chromate conversion coatings. Plasma polymers improve strength and durability of the interface in a fundamentally different way from conventional pretreatments. Whereas conventional metal pretreatments generally function by electrochemical inhibition of corrosion, plasma polymerized primers function as a physical barrier between the interface and the environment.

The variables that affect the properties of plasma polymers include the substrate chemistry and monomer chemistry, as well as plasma parameters such as excitation frequency, power, pressure, and gas flow rate. These plasma parameters all interact to one degree or another to affect the gas phase composition, substrate temperature, and ion kinetic energy, which directly determine the plasma polymer structure and deposition rate. The effect of some of these parameters on the structure and properties of plasma polymerized silica and the relationship between this structure and the resulting strength and durability of adhesive joints is the subject of the current investigation.

Previous work on the composition and morphology of these films has provided substantial evidence as to the chemical and physical origins of the adhesion enhancement seen when they are used as primers. Part of this enhancement is due to the excellent adhesion of the plasma polymerized silica-like films to the metal oxide. Surface analysis using XPS and reflection-absorption FTIR (RAIR) has provided evidence for primary chemical bond formation at this interface [10,11]. This work showed that failure in adhesive joints primed with

plasma polymerized SiO_2 was always either cohesive within the adhesive or very near the adhesive/primer interface: the PP-SiO_2/metal oxide interface was very robust, even under aggressive aging conditions. The impermeability of the films imparted significant corrosion protection to the substrate. Electron microscopy showed these films to be quite rough on a nanometer scale, which provides for interpenetration and mechanical interlocking with the adhesive. Extensive studies using reflection-absorption infrared spectroscopy (RAIR) and X-ray photoelectron spectroscopy (XPS) showed that the surfaces of these plasma polymers were rich in silanol groups that provided for excellent wetting and strong interaction with the adhesive, primarily through hydrogen bonding [10].

In some instances, derivatization of the silanol-rich surface of PP-SiO_2 with organosilanes prior to bonding can significantly improve the hot-wet performance of these primers through chemical modification of the PP-SiO_2/adhesive interface [2]. These results show that the chemical composition of the surface of the plasma polymerized films is critical to adhesive joint durability.

The structure of PP-SiO_2 is controllable over a wide range through control of the deposition conditions. The current work discusses the effect of deposition conditions on structure, and shows that adhesive joint performance is not a strong function of this structure. However, the adhesive joint performance is a strong function of curing agent chemistry. In particular, primary amine-based curing agents can catalyze hydrolysis of the PP-SiO_2 under hot/wet conditions to result in failure close to the primer/adhesive interface within the PP-SiO_2 layer. This failure does not occur when the adhesive is cured with dicyandiamide, however, and these adhesive joints show excellent durability.

The first phase of the study focused on establishing the effect of various deposition parameters on the structure of the resulting plasma polymers. The effects of power, pressure, and sample location relative to the powered electrode on film structure and deposition rate were studied. In addition to establishing first-order effects of these variables in film deposition, this phase of the project established appropriate recipes for testing the effects of film structure on adhesive joint performance later in the study.

Power

Increasing power levels at constant flow rate increases the density of active species in the plasma, increases the substrate bias (and, hence, the kinetic energy of the bombarding species), and increases the level of sample heating. In general, these effects combine to produce films

that have well annealed structures with lower levels of non-bridging oxygen and better mechanical properties. Films such as these may function well as diffusion barrier layers or scratch-resistant layers, but may lack the reactive sites and defects or pores useful as anchor points for adhesives and paints.

Pressure

Several important changes occur in the plasma characteristics as a function of pressure, primarily due to changes in the mean free path of the active gas species Lower pressure increases the volume of the active glow region in the plasma and produces higher average ion kinetic energy due to an increase in the mean free path. Lower pressure also decreases the mean residence time of gas-phase species. This changes the gas composition by increasing the probability of dissociation in the plasma.

Location Within Reactor

Plasmas are not homogenous within a given reactor. Deposition rates and ion bombardment tend to be highest both within and immediately downstream of the active glow region of a reactor (although, at high power levels, deposition within the active glow region may be replaced by etching). The volume of the active glow region increases directly with power level and inversely with pressure. Because of the potential for important effects on polymer structure, knowledge of the effect of sample location within the reactor is very important for scale-up of these processes. Substrates placed on the powered electrode, charged negatively to several hundred volts during plasma deposition due to electron bombardment, show primarily etching and little, if any, film growth. Substrates placed on the ground electrode, charged much less negative with respect to the plasma than the powered electrode, are located within the active glow region where there is a high concentration of short-lived plasma species. This location generally shows the highest growth rates. Substrates that are out of the active glow region are subjected to the minimum ion bombardment and show the least heating, but also show the slowest film growth rates. Plasma polymer is deposited in all locations within a given reactor, but with different rates and different polymer structure.

Analysis of Film Structure

The reflection-absorption infrared spectra of sub-micron silica-like films are characterized by few bands but are sensitive to structure of

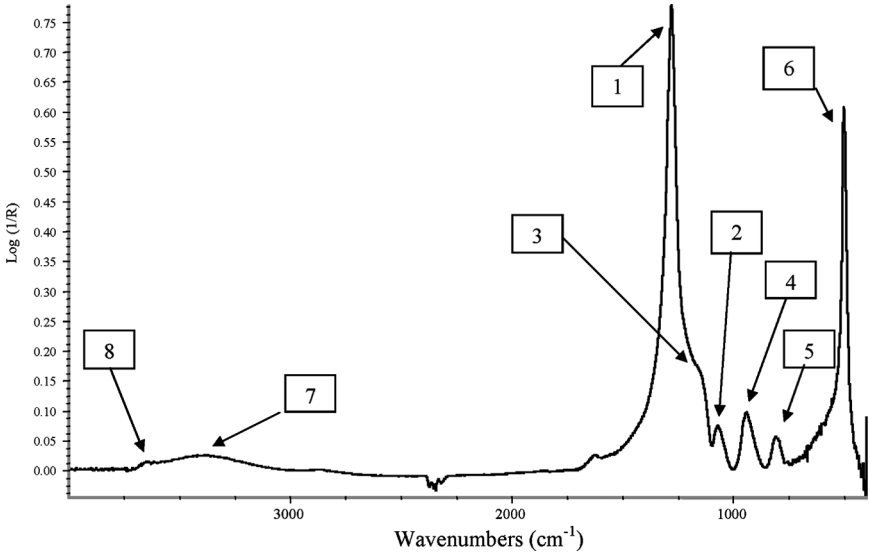

FIGURE 1 Representative FTIR reflection-absorption spectrum of plasma polymerized SiO_2.

the films and provide an excellent tool for analysis. Figure 1 shows a representative spectrum obtained at an average incidence angle of 80°, and Table 1 shows the location and assignments of the major features [12,13]. The location of the strongest spectral feature, due to an Si-O-Si asymmetric stretching vibration, depends upon the sample thickness and the sampling technique used. In reflection spectra obtained at grazing angles of incidence, the longitudinal optical (LO) phonon associated with this vibration is active and appears near

TABLE 1 Band Assignments for Spectrum in Figure 1, from [13–15]

Band identifier	Location (cm^{-1})	Assignment
1	1250	Si-O-Si asymmetric stretch (AS1), LO mode
2	1075	Si-O-Si asymmetric stretch (AS1), TO mode
3	1180	Si-O-Si asymmetric stretch (AS2), TO + LO modes
4	945	Si-O stretch, non-bridging oxygen
5	502	Si-O-Si rocking
6	810	Si-O-Si symmetric stretch
7	3350	O-H stretching, adjacent H-bonded
8	3600	O-H stretching, isolated

$1250\,cm^{-1}$. As film thicknesses increase beyond about $0.1\,\mu m$, the transverse optical (TO) phonon associated with this vibration begins to appear near $1075\,cm^{-1}$. For film thicknesses of approximately $1\,\mu m$ or more, the TO phonon begins to dominate the spectrum, which takes on the characteristics of a transmission spectrum due to the long path length of the incident and reflected beams through a film whose thickness is approaching the wavelength of light. Other spectral features include an Si-O-Si rocking mode near $500\,cm^{-1}$ and a bending mode near $860\,cm^{-1}$.

In general, films of SiO_2 obtained by plasma polymerization under the conditions used in this study contain significant concentrations of network imperfections in the form of non-bridging (or dangling) oxygens. The presence of non-bridging oxygens gives rise to an absorbance in the infrared spectra near $940\,cm^{-1}$ attributed to the Si-O stretching vibration [13,14]. While these oxygens may exist as radical species, the quantity of hydrogen released by cleavage of the organosilicon precursor during polymerization and the exposure of the films to atmospheric moisture after deposition ensures that most of these radicals will be quenched to form silanols. Two types of silanols are identifiable by distinct spectral features in the O-H stretching region of the IR spectrum [14]. Silanols that are physically isolated from other silanol groups appear as a sharp feature near $3600\,cm^{-1}$. Silanols that are hydrogen bonded to other silanols appear as a broader, more diffuse feature centered near $3350\,cm^{-1}$. As these silanols probably represent the reactive sites for attachment of adhesives or paints, the nature and concentration of these groups is potentially very important.

Reflection FTIR spectra are representative of the structure of the film averaged over the entire thickness. To complement this information, variable angle X-ray photoelectron spectroscopy was used to characterize the chemistry and composition of the uppermost 1–10 nm. In addition to quantifying the atomic composition of the sample surfaces, much information about the chemistry of these regions was obtained. Because of changes in the core-level binding energies associated with different valence level bonds, the level of oxidation of the silicon can be readily detected [15]. Furthermore, the presence of hydroxyl groups is characterized by changes in the O(1s) binding energies which can be quantified through curve fitting of the high-resolution core level spectra [16].

After establishing the effects of deposition parameters on film structure, adhesive joints were prepared with two different adhesives to determine the effect of polymer structure on adhesive performance. A simple polyamide amine cured epoxy formulation was used as an example of a class of adhesives that is both commercially important

as well as potentially capable of chemically interacting with (slightly acidic) silanols in a manner that could be either beneficial or detrimental to adhesive joint performance. Results with this adhesive were compared with a commercial dicyandiamide cured epoxy system, shown previously [1] to perform particularly well with similar plasma-polymerized primer systems.

EXPERIMENTAL

Sample coupons of ferrotype plate (1×3 in chrome-plated steel) (2.5×7.6 cm) were used as witness coupons for investigating film structure and deposition rate. This material is highly reflective, clean, and inexpensive, making it an attractive substrate for reflection IR and XPS investigations. It is recognized that the substrate composition can have a profound effect on the structure of the plasma polymer close to the substrate-plasma polymer interface [17], but the effect of substrate composition on the infrared spectra of the films seems to be minimized for thick films ($> ca.$ 100 Å). These were cleaned with acetone prior to inserting in the reactor. All depositions were preceded by a 5 to 10 min exposure to an oxygen plasma to ensure substrate cleanliness. In work using a plasma reactor attached to the sample introduction chamber of an XPS, the author has found that this procedure provides a surface that is reproducibly clean at the atomic level prior to plasma polymer deposition.

The plasma reactor used was an Advanced Plasma Systems (se Petersburg, FL, USA) capacitively coupled RF instrument (13.56 MHz), configured as shown in Figure 2. In this configuration, the oxygen inlet is uppermost in the reactor, followed by the powered and ground electrodes, the monomer inlet, and finally at the bottom of the reactor a perforated plate used as a sample stage for depositions. Below this perforated plate were the exhaust ports. This arrangement was used to establish a "downstream" configuration to maximize deposition efficiency by ensuring that the bulk of the plasma polymer deposition would occur below the electrodes where the samples were located. Films of SiO_2 were deposited from mixtures of oxygen and hexamenthyldisiloxane(HMDSO). In order to separate the effects of pressure from those of gas residence time in the plasma, the total flow rate was adjusted to maintain a constant gas residence time of 5 seconds at both pressures investigated. The average gas residence time was calculated as the quotient of active plasma volume and flow rate [18], with the active plasma volume calculated to be 14.5 l (based on visual observation of the active plasma region occupying approximately

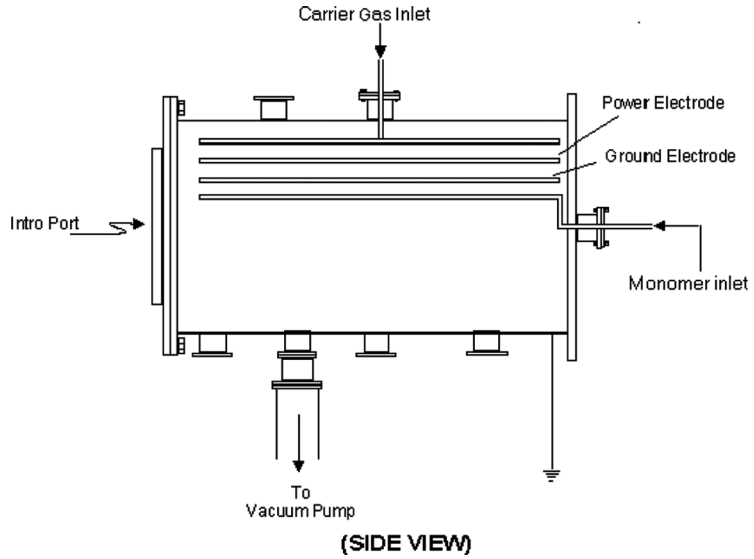

FIGURE 2 Layout of RF reactor used in deposition parameter experiments.

the upper 13 cm of the chamber). Table 2 shows the range of parameters investigated.

Overall film structure was studied using fourier transform infrared spectroscopy (FTIR). Grazing angle spectra were obtained with a Nicolet Magna 760 FTIR equipped with a Nicolet FT-80 reflection accessory (Thermo Scientific, Waltham, MA, USA). Film thicknesses were measured using a Woollam spectroscopic ellipsometer and WVASE software (J. A. Woolam, Inc., Lincoln, NE, USA). Surface compositions were studied using variable angle X-ray photoelectron spectroscopy

TABLE 2 Deposition Parameters Used in RF Reactor for Figures 3–9

Constant parameters	Power (W)	Pressure (Torr)	Sample location in reactor	Film thickness (Å)
95% O_2	150	0.500	A: Ground electrode	2100
5% HMDSO			B: Reactor floor	840
5 sec gas	200	0.500	C: Ground electrode	1920
residence time			D: Reactor floor	1740
30 min deposition time			E: Reactor floor, ground electrode removed	2160
		0.150	F: Ground electrode	1890
			G: Reactor floor	1170

(XPS). XPS spectra were collected using a Physical Electronics 5400 XPS (MgKα radiation, 300 W/1500 kV, Chanhassen, MN). Resolution of overlapping components in the core level O(1s) and Si(2p) spectra was accomplished through the use of well established curve fitting procedures. These are based on peak widths, peak shapes, and peak locations obtained from spectra of well characterized standard materials that were analyzed in the same instrument under the same experimental conditions.

To evaluate the effect of PP-SiO_2 film structure and composition, lap joints were constructed as per ASTM D1002 specifications using type 6111 aluminum coupons as substrates. The coupons were cleaned in acetone and deoxidized in Aldeox 171 (A. Brite Co., Garland, TX, USA) prior to further processing. One set of adhesive joints was constructed using Ciba-Geigy AV-3131 automotive adhesive (a one-part formulation based on dicyandiamide cure chemistry) (Tarrytown, NY, USA) while another set was constructed using Epon 828® (liquid DGEBA epoxy resin) with Epi-cure 3140® (amine-terminated polyamide) (Miller-Stephenson Chemical Company, Morton Grove, IL, USA as the curing agent. Recommended concentration ranges (parts per hundred of resin, phr) as per manufacturer's recommendations ranged from 33–133 phr; lower ratios lend a more brittle nature to the adhesive joint and higher ratios make the joint more flexible. Several ratios were tested to determine the optimum for this investigation. It was established that 150 phr gave the optimum breaking strength and elongation to failure and were used in construction of adhesive test specimens; these specimens failed cohesively within the adhesive. Lap joints of Epon 828/V3140 were cured overnight at room temperature then postcured at 100°C for 1 hour. Those constructed using AV-3131 were cured 45 min at 60°C. Adhesive joints were evaluated for strength and failure mode using conditions outlined in ASTM D1002.

RESULTS AND DISCUSSION

Figures 3 through 9 represent the RAIR spectra obtained from samples A through G in Table 2.

Effect of Sample Location in Reactor

The active plasma zone (identified by visible glow) is located close to the powered electrode in the uppermost part of the reactor. At pressures near 0.500 torr, this zone is confined to the region within a few centimeters of the powered electrode by the limited mean free path of the active gas species. At the lower pressure of 0.150 torr, the size

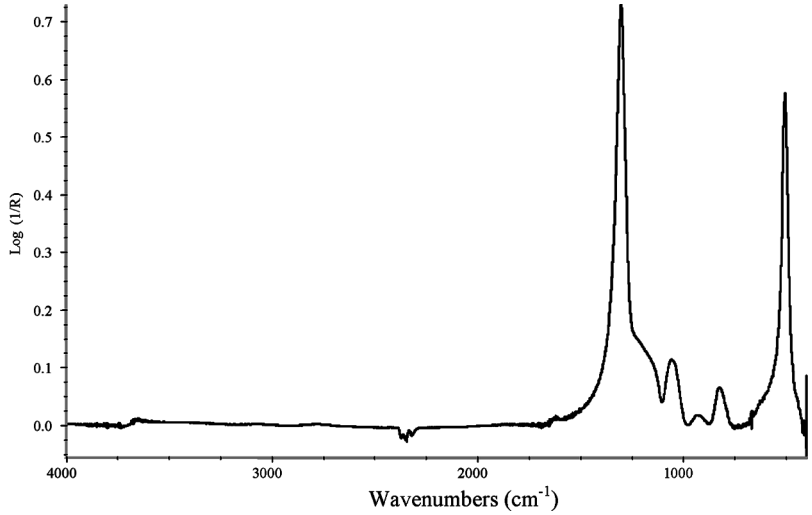

FIGURE 3 Sample A, plasma polymerized SiO_2.

of the active glow region increased noticeably, but still did not extend to the reactor floor where the other samples were located. Samples on the reactor floor were, therefore, always out of the active glow region, while those on the ground electrode were within the active glow

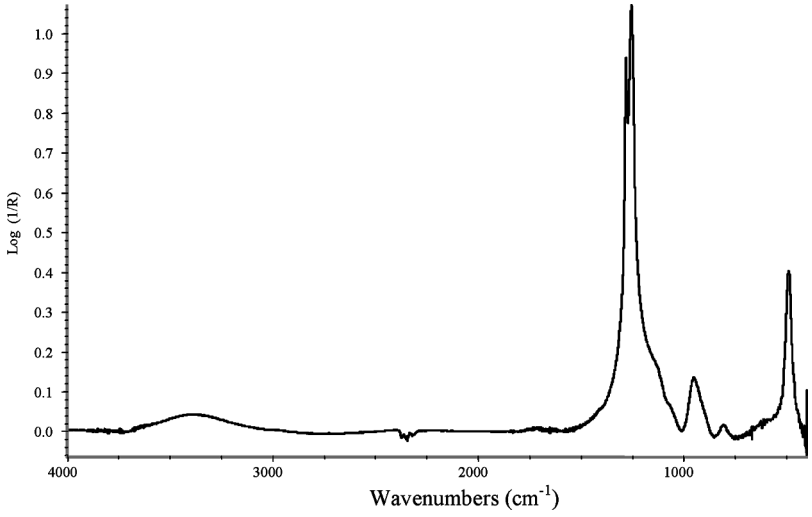

FIGURE 4 Sample B, plasma polymerized SiO_2.

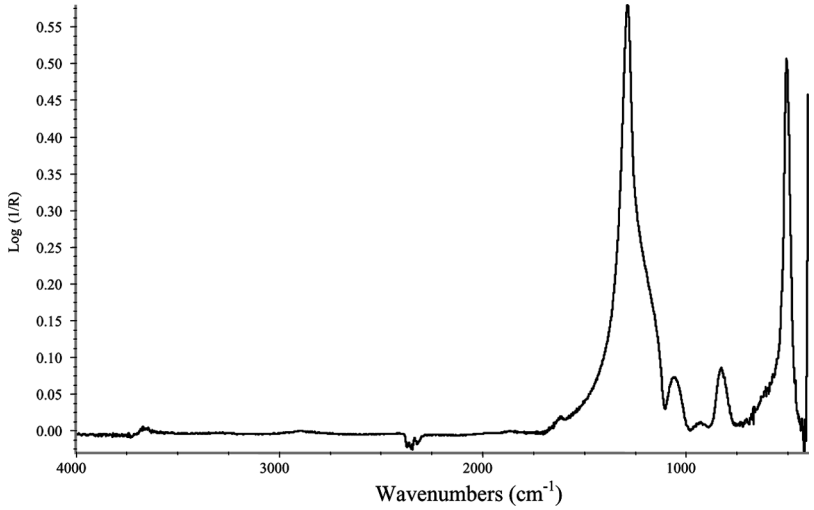

FIGURE 5 Sample C, plasma polymerized SiO_2.

region. Comparison of Figures 3–9 show that the samples from the reactor floor invariably had a higher fraction of hydroxyl content as shown by bands due to O-H stretching near 3350 cm^{-1} and Si-O stretching near 940 cm^{-1}.

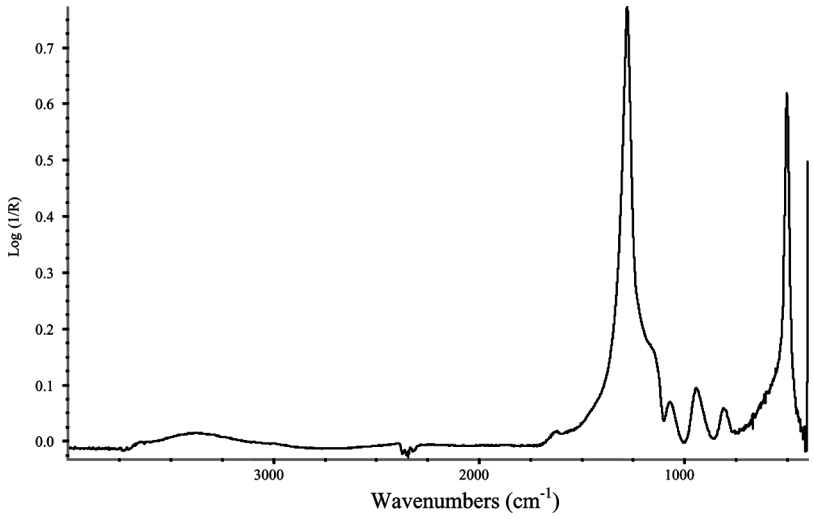

FIGURE 6 Sample D, plasma polymerized SiO_2.

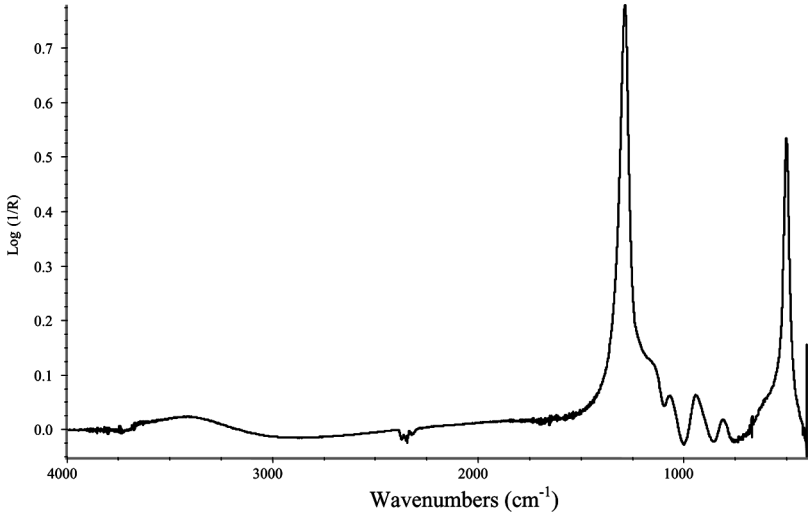

FIGURE 7 Sample E, plasma polymerized SiO_2.

Figure 7 was obtained from a sample located on the reactor floor, but with the ground electrode removed. Comparison with Figure 6 (deposited under identical conditions but with the ground electrode present) shows that the ground electrode has little or no detectable

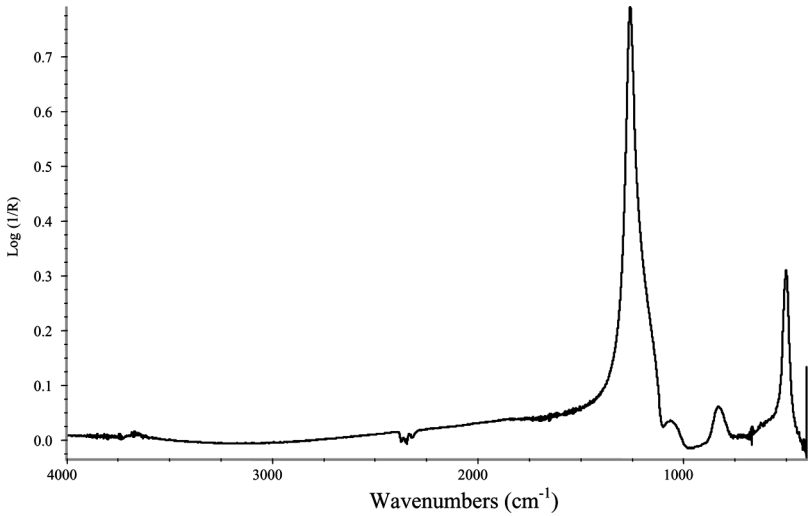

FIGURE 8 Sample F, plasma polymerized SiO_2.

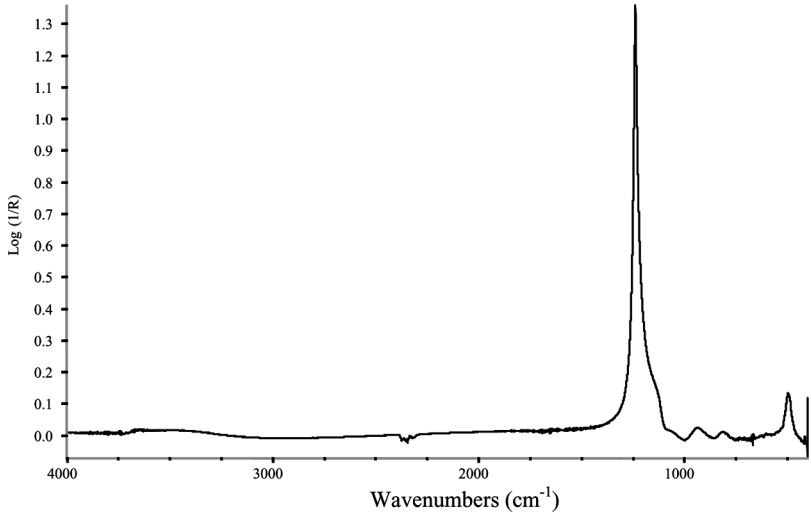

FIGURE 9 Sample G, plasma polymerized SiO_2.

effect in these depositions. The proximity of the chamber walls to the powered electrode probably provides the most active ground plane for establishment of the electric field.

Effect of Power Level

150 and 200 watts were investigated. These are both relatively high powers, but due to the high monomer fraction in the gas mixture (5%), higher powers are necessary to ensure complete fragmentation and crosslinking. Figures 3 and 4, obtained at the lower power level, show the effect of insufficient fragmentation. While the sample on the ground electrode (Figure 3) looks like a normal SiO_2 film with relatively high hydroxyl content, the sample located on the reactor floor (Figure 4) has a sharp peak at 1275 cm^{-1} due to the Si-CH_3 symmetric C-H deformation of incompletely dissociated HMDSO [19]. The assignment of this band is corroborated by the presence of absorbance in the C-H stretching region near 2800 cm^{-1}. The lack of sufficient ion kinetic energy at this location and power level produced a film with significant carbon content. None of the other spectra show this feature.

Effect of Pressure

Figures 8 and 9 were obtained from samples deposited at 0.150 torr pressure instead of 0.500 torr. The flow rate was adjusted in these

depositions to maintain a constant gas residence time in the reactor. The sample from the active glow region (Figure 8) shows the least hydroxyl and non-bridging oxygen of all the samples investigated, while the sample from the reactor floor (Figure 9) shows significantly less hydroxyl than the corresponding samples deposited at higher pressure. The longer mean free path at this pressure allowed higher ion kinetic energy to anneal the films during growth and reduce the hydroxyl content.

This represents a first-order analysis of spectra-structure correlations in plasma polymerized SiO_2. There are other features in these spectra, however, whose origins are not as clear. For example, the relative contribution of the AS2 LO-TO pair near 1180 cm^{-1} (see Figure 1 and Table 1) varies in these spectra. The spectra in Figures 5 and 8 show a much more prominent feature in this region than the other spectra. The intensity in this region has been related to mode coupling between the AS1 and AS2 vibrational modes, and disorder in the structure is believed to increase the degree of coupling and, therefore, increase the optical strength of this mode [12].

Scratch Resistance as a Function of Deposition Conditions

The samples from Table 2 were subjected to a scratch hardness test using an increasing load scratch hardness tester equipped with a 120° conical diamond indenter and an loading rate of 1 N/mm. All films except sample D (high power, active plasma zone) showed quite brittle behavior, cracking from the substrate at a load as low as 2 N. Sample D showed resistance to perhaps 10 N before failure occurred.

Electron microscopy of the scratch of these films showed excellent adhesion to the aluminum surface. Figure 10 shows a picture of a scratched region. The spherical morphology of the plasma polymer is clear, and is expected for depositions performed at temperatures well below the melting point of the film-former [18]. Of great interest are the substrate features that appear to be promulgated through the growing plasma polymer film and replicated on the upper surface.

Effect of Surface Chemistry of Plasma Polymerized SiO_2 on Adhesive Joint Strength and Failure Mode

In order to relate plasma polymer structure to primer performance, depositions were performed on 6061-T3 aluminum adherends prior to adhesive bonding. Films with two distinct structures were investigated: high hydroxyl content was obtained using relatively high

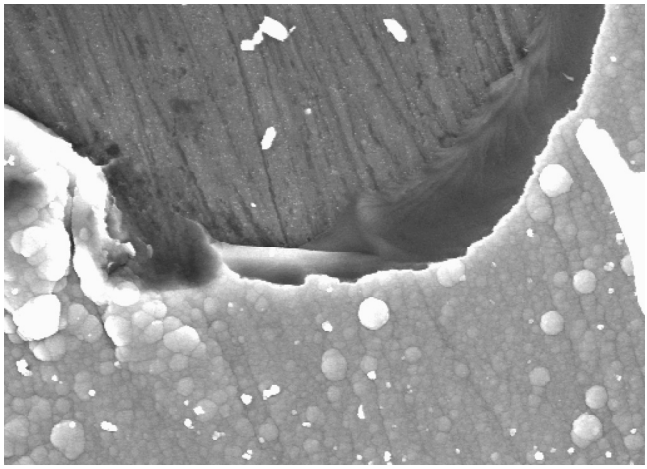

FIGURE 10 Aluminum substrate, plasma polymerized SiO_2. Upper part of picture is substrate revealed by scratch test.

pressure and high monomer/oxidizer ratios, and low hydroxyl content was obtained using lower pressure and lower monomer/oxidizer ratio. Table 3 shows the deposition conditions used in these experiments.

Reflection-absorption FTIR spectra obtained from these samples are shown in Figures 11 and 12. The film obtained using low pressure and low monomer flow (Figure 11) has a much lower overall hydroxyl content than the film obtained at higher pressure and higher monomer flow (Figure 12). Figure 13 shows an expanded presentation of the hydroxyl O-H stretching regions for comparison. The low pressure/lean mixture regime produced a film with much less total hydroxyl. However, the peak near 3600 cm^{-1} due to isolated hydroxyls is still present in this spectrum.

Figure 14 shows an expanded presentation of the Si-O regions for comparison. The spectra obtained from these films show that the

TABLE 3 Deposition Parameters Used in RF Reactor for Figures 11–14 (Flow Rates Were Adjusted to Obtain a 5 Second Gas Residence Time. Depositions Were 30 Minutes Each)

Goal	Power (W)	Gas ratio	Pressure (Torr)	Film thickness (Å)
High-OH	150	95:5	0.500	2100
Low-OH	150	98:2	0.150	600

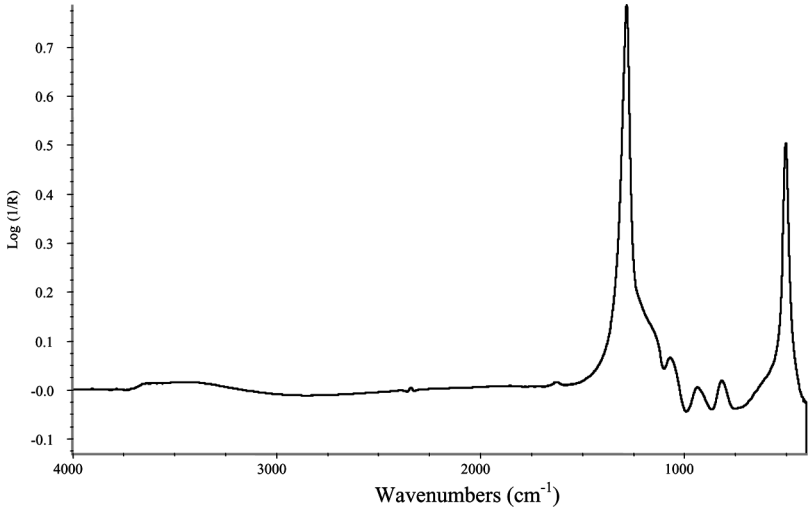

FIGURE 11 Plasma polymerized SiO_2 deposited under conditions resulting in high hydroxyl content (Table 3).

intensity of the AS2 LO-TO pair (shoulder near 1200 cm^{-1}) is inversely proportional to the relative amount of non-bridging oxygen (940 cm^{-1}). According to Kirk [12], the intensity of the AS2 LO-TO band is an

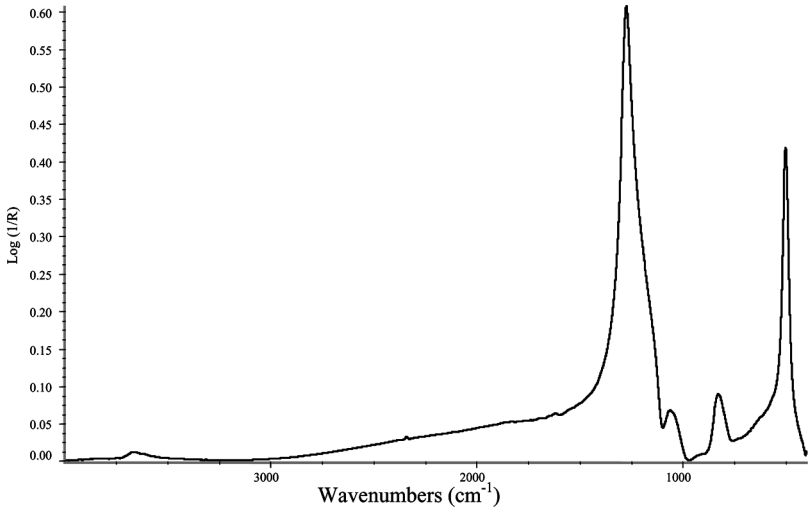

FIGURE 12 Plasma polymerized SiO_2 deposited under conditions resulting in low hydroxyl content (Table 3).

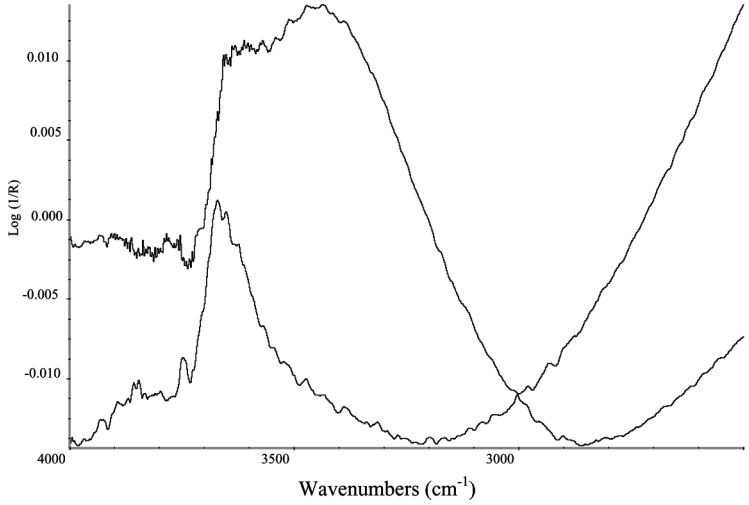

FIGURE 13 Expanded -OH region for spectra in Figures 11 and 12. Top: 95/5 O_2/HMDSO, Bottom: 98/2O_2/HMDSO. Conditions from Table 3.

indicator of relative disorder in the films. Because non-bridging oxygens represent points of imperfection in the SiO_2 network, it was expected that the amount of non-bridging oxygen would also correlate

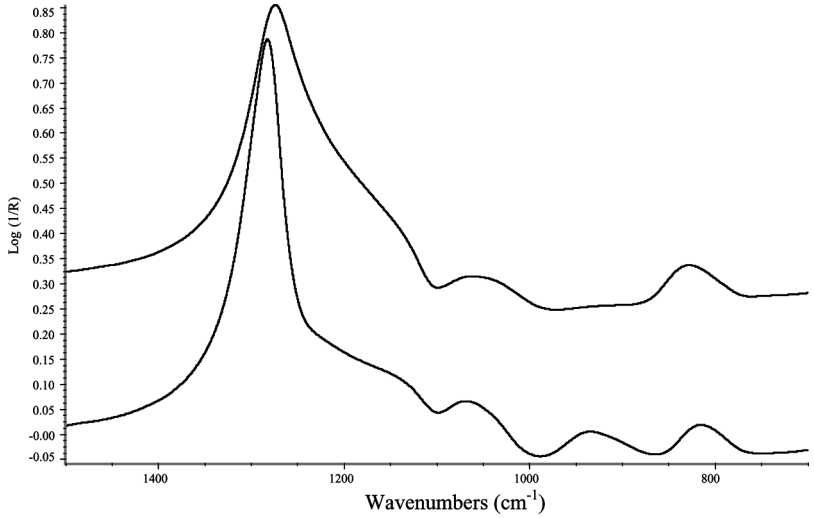

FIGURE 14 Expanded Si-O region for spectra in Figures 11 and 12. Top: 95/5 O_2/HMDSO, Bottom: 98/2O_2/HMDSO. Conditions from Table 3.

to the relative disorder. These data suggest that the relative amount of disorder does not correlate to the amount of non-bridging oxygen, however. Structural disorder is potentially important: highly ordered networks may be physically stronger and have superior barrier properties. Less ordered networks may have more free volume for resin interpenetration as well as more reactive attachment sites for adhesive/substrate interaction or for chemical derivatization.

XPS analysis of these films was performed to determine if the differences in overall film structure detected using FTIR translated into detectable differences in surface chemistry.

Table 4 shows the atomic composition of the as-deposited films.

XPS analysis showed the films to consist of silicon, oxygen, and carbon with several atomic percent of fluorine. No chromium was detected, confirming that the films were continuous and thicker than the escape depth of the Cr photoelectrons. Both films showed an excess of oxygen over stoichiometric SiO_2. Silicon and oxygen were present in approximately a 1:2.4 ratio for the higher hydroxyl content films, and a 1:2.2 ratio for the low hydroxyl films. Each non-bridging oxygen contributes one additional oxygen to the network. These data show that the films are composed of imperfect SiO_2, and that films whose FTIR spectra show increased non-bridging oxygen also have a greater excess of oxygen over stoichiometric SiO_2.

The decrease in the carbon and fluorine signals with increasing exit angle indicate that these are present on the surface of the plasma polymer. The fluorine and some of the carbon were probably due to contamination from the fluorinated polyether vacuum pump oil necessary for plasma processes that involve oxidizing gases.

Further information was obtained from the shape of the O(1s) spectra. As discussed above, FTIR spectra clearly identified a range of hydroxyl content in these films. Hydroxyl-terminated SiO_2 has a distinct O(1s) component in the XPS spectra [15,16], and this component

TABLE 4 Atomic Composition of As-Deposited Films from Table 3 as Measured by XPS

Sample	Exit angle	Si	O	O/Si	C	F	Al	N
95/5O_2/HMDSO	15°	26.4	62.3	2.36	7.0	3.6	–	–
	38°	26.4	63.8	2.42	6.5	3.1	–	–
	75°	26.3	65.4	2.49	5.5	2.5	–	–
98/2O_2/HMDSO	15°	24.2	52.4	2.17	19.0	3.0	–	–
	38°	24.6	55.0	2.24	16.2	2.8	–	–
	75°	25.7	57.2	2.23	14.2	2.1	–	–

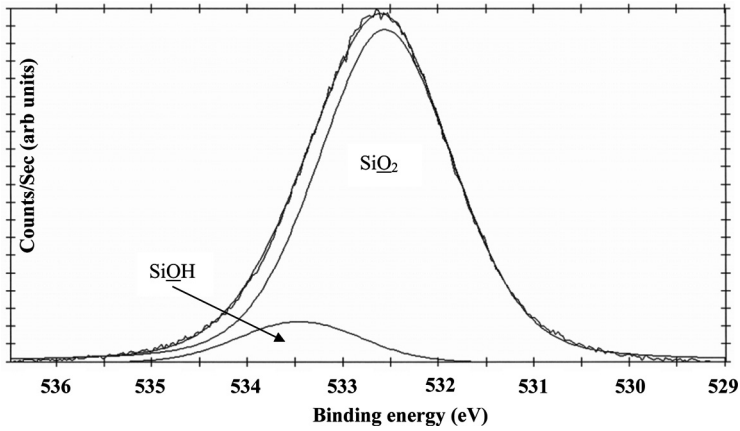

FIGURE 15 O(1s) XPS spectrum, $95/5O_2$/HMDSO film, 15° exit angle.

was detectable through curve-fitting of the corresponding O(1s) spectra. A representative spectrum is shown in Figure 15, and the relative amounts of these species measured in each sample is shown in Table 5. These data show that the relative amount of hydroxyl is decreasing with exit angle, consistent with a higher concentration of hydroxyls on the upper surface of the plasma polymerized SiO_2.

Plasma polymerization proceeds by chemisorption of largely intact gas-phase species onto a plasma activated surface, followed by fragmentation and rearrangement of the sorbed species through processes such as ion bombardment and UV irradiation. Film growth occurs as gas phase species sorb and react onto this initial layer. The immobilized species are subjected to additional bombardment, fragmentation, and rearrangement until the film has grown to a sufficient thickness to shield it from further effects of the plasma. The result is a gradient

TABLE 5 Relative Amounts of SiO_2 and SiOH as Determined by O(1s) Curve Fits for Films Described in Table 3

Sample	Exit angle	SiO_2	SiOH
$95/5O_2$/HMDSO	15°	88.1	11.9
	38°	90.0	10.0
	75°	91.1	8.9
$98/2O_2$/HMDSO	15°	87.1	12.9
	38°	89.8	10.2
	75°	92.1	7.9

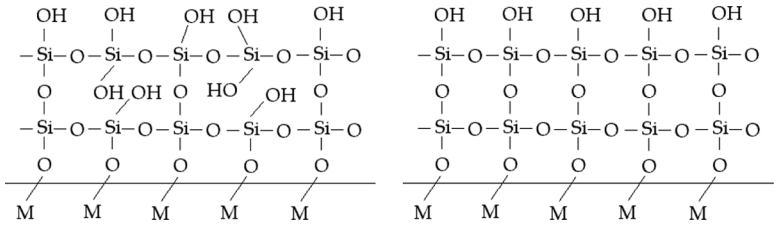

FIGURE 16 Structural representations of plasma polymerized SiO_2 films on metal substrates. Left: films obtained from high HMDSO/oxygen ratios at higher pressures; Right: films obtained using lower HMDSO/oxygen ratios at lower pressures. M represents metal oxide surface.

film structure, whereby the outermost layers of the film have seen the shortest exposure to the plasma, the least effect of ion bombardment, and the greatest structural imperfection. The uppermost surface is expected to show the highest concentration of non-bridging oxygen in the form of hydroxyl.

These data allow a fairly complete picture of the structure of the plasma polymerized SiO_2 to be established as a function of deposition conditions. Models representing these structures are shown in Figure 16. Low ratios of oxygen to HMDSO (such as 95/5) and higher pressures produce films with more structural imperfection, manifested as non-bridging oxygens terminated in hydroxyl groups. Higher ratios of HMDSO to oxygen and lower pressures produce films with a higher degree of structural perfection. Hydroxyls are present in the uppermost portions of both types of plasma polymerized films.

Adhesive Joint Performance

The effect of hot/wet aging on adhesive strength and failure mode is shown in Table 6. The failure mode of the joints prepared using the dicyandiamide cured adhesive was cohesive within the adhesive for both unaged and aged joints, showing that the aging conditions were not aggressive enough to distinguish any effect from the plasma polymerized SiO_2 pretreatment. The situation with the amine cured adhesive was different, however. While the failure mode of the joints prepared with this adhesive was cohesive within the adhesive prior to hot/wet aging, the failure locus shifted with aging to a visually interfacial mode. This was in agreement with previous experiences [1] and indicated that the interface between the amine cured epoxy and the plasma polymerized SiO_2 is sensitive to moisture. The aluminum coupon maintains a bright appearance during the aging process,

TABLE 6 Breaking Strength (psi) and Failure Mode of Adherends Primed with Plasma Polymers Per Table 3 (Aging Conditions: Three Weeks/60°C Water Immersion)

	Polyamide amine cure				Dicyandiamide cure			
	Unaged		Aged		Unaged		Aged	
Plasma polymer	Strength (psi)	Failure mode	Strength (psi)	Failure mode	Strength (psi)	Failure mode	Strength (psi)	Failure mode
95/5	2198	cohesive	1532	adhesive	2858	cohesive	2998	cohesive
98/2	2038	cohesive	1498	adhesive	3735	cohesive	3231	cohesive

however, showing that the plasma polymer protects the substrate from corrosion.

XPS analysis was undertaken of the failure surfaces from the joints prepared using the amine cured adhesive to determine the locus of failure on a molecular level. Table 7 shows the atomic composition of the fracture surface obtained from one of the samples.

Silicon (from the plasma polymer) and nitrogen (from the curing agent) were detected on both sides of the fracture surface, showing that the adhesive joint failed in a zone of interpenetrated adhesive and primer. Closer inspection of the spectra from these elements showed that the SiO_2 on the epoxy side was less well crosslinked than on the aluminum side, and that approximately 30% of the amine in this region was protonated to NH_3^+.

Tetrahedral SiO_4 is susceptible to nucleophilic attack by ^-OH to form a five-coordinated intermediate that decomposes through rupture of the Si-O-Si bond [20]:

$$\text{Si-O-Si} + {}^-\text{OH} \rightarrow \text{Si-O}^- + \text{Si(OH)}.$$

TABLE 7 Atomic Composition of Fracture Surfaces as Measured by XPS from Adhesive Joint Prepared using $98/2O_2$/HMDSO and Bonded with Polyamide Amine Cured Epoxy

Surface	Exit angle	Si	O	C	F	Al	N
"Metal" side	15°	4.1	26.2	62.4	2.0	0.9	4.4
	38°	6.5	28.5	57.2	1.7	1.3	4.8
	75°	7.6	30.6	54.9	1.0	0.7	6.1
"Adhesive" side	15°	1.3	9.5	79.5	3.1	0.7	6.0
	38°	1.3	10.2	79.7	1.3	0.8	6.7
	75°	1.6	10.6	80.0	1.0	0.7	6.1

This reaction is slow for pure silica, where formation of the five-coordinated intermediate is inhibited by the high connectivity of the network. The presence of non-bridging oxygen makes the five-membered intermediate sterically easier to form and the degradation is enhanced. Hydrolysis is also enhanced by a high pH environment. It is apparent that in the presence of an amine curing agent, hot/wet aging resulted in hydrolysis and weakening of the plasma polymerized $SiOU_2$ so that failure occurred in an interpenetrated region of adhesive and primer. Derivatization of the plasma polymer with appropriate organofunctional modifiers consumes the non-bridging oxygens through creation of organosilicon esters and prevents this weakening process [2,21].

CONCLUSIONS

Plasma polymerized SiO_2 creates a covalently bound barrier coating on aluminum surfaces that can prevent corrosion and provide an excellent substrate for adhesion of an organic adhesive or paint. Structural imperfections in the network, such as non-bridging oxygens and terminal hydroxyls, are readily detectable by XPS and FTIR, and the relative degree of network perfection is controllable through manipulation of deposition parameters. Slower film growth (through leaner monomer/oxidizer ratios) under conditions of higher ion bombardment energy (through lower pressures, higher power, or placement within the reactor) produces a network with fewer imperfections.

These imperfections have little effect on dicyandiamide cured adhesives, and plasma polymerized SiO_2 is an excellent pretreatment for adhesive bonding with these systems that shows little sensitivity to details of film structure. However, when amine cured adhesives are used, hot/wet aging results in failure within a region of interpenetrated silica and adhesive that is weakened due to base catalyzed hydrolysis. If these network imperfections are consumed by derivatization prior to adhesive bonding, network degradation is inhibited and excellent joint strength and durability is obtained with amine cured systems.

REFERENCES

[1] Dillingham, R. G. and Boerio, F. J., *Proc. 22nd Annual Meeting of the Adhesion Society*, D. R. Speth (Ed.) (The Adhesion Society, Inc., Blacksburg, VA, 1999), pp. 7–9.
[2] Turner, R. H., Segall, I., Boerio, F. J., and Davis, G. D., *J. Adhesion* **62**, 1–21 (1997).
[3] Taylor, C. E., Segall, I., Boerio, F. J., Ondrus, D. J., Ward, S. M., and Dickie, R. A., *Proc. 18th Annual Meeting of the Adhesion Society*, J. W. Holubka (Ed.) (The Adhesion Society, Inc., Blacksburg, VA, 1995), pp. 95–97.

[4] daSilva Sobrinho, A. S., Latréche, M., Czeremuszkin, G. E., Klemberg-Sapieha, J. E., and Wertheimer, M. R., *J. Vac. Sci. Technol. A* **16** (6), 3190–3198 (1998).
[5] Yasuda, H. K., *Plasma Polymerization*, (Academic Press, Orlando, FL, 1985).
[6] d'Agostino, R., *Plasma Deposition, Treatment and Etching of Polymers*, (Academic Press, San Diego, CA, 1990).
[7] Boenig, H. V., *Fundamentals of Plasma Chemistry and Technology*, (Technomic Publishing Co., Lancaster, PA, 1988).
[8] Auciello, O. and Flamm, D. L., *Plasma Diagnostics: Volume 1: Discharge Parameters and Chemistry, Volume 2: Surface Analysis and Interactions*, (Academic Press, San Diego, CA, 1989).
[9] Yasuda, H. K., *Plasma Polymerization and Plasma Treatment of Polymers, Applied Polymer Symposia 42*, (John Wiley & Sons, New York, 1988).
[10] Turner, R. H. and Boerio, F. J., *J. Adhesion* **78**, 447–464 (2002).
[11] Turner, R. H. and Boerio, F. J., *J. Adhesion* **78**, 465–493 (2002).
[12] Kirk, C. T., *Phys. Rev. B* **38**, 1255–1273 (1988).
[13] Theil, J. A., Tsu, D. V., Watkins, M. W., Kim, S. S., and Lucovsky, G., *J. Vac. Sci. Technol. A* **3**, 1374–1381 (1990).
[14] Theil, J. A., Tsu, D. V., and Lucovsky, G., *J. Electron Mater.* **19**, 209–217 (1990).
[15] Barr, T. L., *J. Phys. Chem.* **82**, 1801–1810 (1978).
[16] McCafferty, E. and Wightman, J. P., *Surf. Int. Anal.* **26**, 549–564 (1998).
[17] Dillingham, R. G., Guo, J., and Boerio, F. J., *Proc. 21st Annual Meeting of the Adhesion Society*, R. A. Dickie (Ed.) (The Adhesion Society, Inc., Blacksburg, VA, 1998) pp. 85–87.
[18] Smith, D. L., *Thin Film Deposition: Principles and Practice*, (McGraw-Hill, NY, 1995).
[19] Colthup, N. B., Daly, L. H., and Wiberley, S. E., *Introduction to Infrared and Raman Spectroscopy*, 2nd ed., (Academic Press, NY, 1975).
[20] Bunker, B. C., J. *Non-Crystalline Solids* **179**, 300–308 (1994).
[21] Boerio, F. J., Wagh, V. H., and Dillingham, R. G., *J. Adhesion* **81**, 115–142 (2005).